Bis-Hydrophilic Block Terpolymers via RAFT Polymerization: Toward Dynamic Micelles with Tunable Corona Properties

Andreas Walther,[†] Pierre-Eric Millard,[†] Anja S. Goldmann,[†] Tara M. Lovestead,[‡] Felix Schacher,[†] Christopher Barner-Kowollik,[‡,§] and Axel H. E. Müller*[,†]

Makromolekulare Chemie II and Bayreuther Zentrum für Kolloide and Grenzflächen, Universität Bayreuth, D-95440 Bayreuth, Germany and Centre for Advanced Macromolecular Design, School of Chemical Sciences and Engineering, The University of New South Wales, NSW 2052, Australia

Received May 31, 2008; Revised Manuscript Received August 22, 2008

ABSTRACT: We present the synthesis of well-defined bis-hydrophilic block terpolymers with two outer hydrophilic blocks and an inner hydrophobic block together with studies concerning their colloidal aggregates formed in water. The investigations aim at preparation of dynamic micelles with tunable corona properties. Highly functionalized poly(ethylene oxide) macro-chain-transfer agents (PEO-CTAs) of two molecular weights (2 and 5 kDa) are used as mediating agents in reversible addition fragmentation chain transfer (RAFT) polymerization. The synthesis is accomplished by first polymerizing *n*-butyl acrylate as a hydrophobic block and then chain extending the diblock copolymers further with various (meth)acrylamide derivatives, acrylamide (AAm), *N*-isopropylacrylamide (NIPAAm), *N*,*N*-diethylacrylamide (DEAAm,) and *N*-(2-hydroxypropyl)methacrylamide (HPMA). Due to the high degree of functionalization of the PEO-CTA, the blocking efficiency is near quantitative and the diblock copolymers can be obtained easily in a wide range of compositions and with an excellent control of the molecular weights and polydispersities (<1.15). Similarly, chain extension with the different (meth)acrylamide proceeds with very high blocking efficiencies to obtain well-defined block terpolymers. The hydrophilic-to-hydrophobic balance as well as the chain lengths of the hydrophilic blocks can be adjusted as desired. The second part of this study describes the aqueous solution characteristics of the micellar aggregates of the block terpolymers. A significant effect of the preparation pathway (direct dissolution or dialysis from a common solvent) on the type of formed aggregates is found, indicating a strong influence of the dissolution kinetics. The self-assembled aggregates are of dynamic character as they can undergo fusion and fission processes, induced by both temperature and time. Large-scale rearrangement of the architectures are possible as ensured by the low glass-transition temperature of the hydrophobic block, poly(*n*-butyl acrylate). Depending on the hydrophilic-to-hydrophobic balance and the pair of hydrophilic end blocks employed, spherical micelles, worm-like micelles, and vesicles can be found. The corona structure of the micelles can be tuned by changing the length and type of hydrophilic polymers used.

Introduction

Block copolymers are able to self-assemble into discrete and well-defined colloidal aggregates in the mesoscopic size range. The significant interest in these structures originates from their potential applications in a variety of fields, such as nanotechnology and biomedicine. Great effort has been directed at the exploration of the aggregate structures of diblock copolymers. In particular, with the introduction of advanced polymerization techniques such as controlled radical polymerization methods it was possible to substantially broaden the accessible structures. At the same time, the concept of "smart" nanoparticles was introduced and led to the discovery of tunable structures as in the case of so-called "schizophrenic micelles".[1−7] "Smart" nanoparticles undergo structural changes while sensing environmental stimuli, such as changes in temperature, pH, or ionic strength.[8−21] With these properties, clearly, applications in the biomedical field have come into the focus and represent some promising approaches for tackling problems in controlled delivery and controlled release of active compounds.[11−13,22−26]

In very recent time efforts have been undertaken to obtain a further subdivision of the micellar structures as in the case of Janus particles[27,28] or other multicompartment micelles.[29−34] These studies are triggered by not only scientific curiosity but also the possibility of reaching novel structures with advanced properties. For instance, multicompartment micelles can provide interesting possibilities in terms of multicomponent storage.[29,35−38] An intrinsic prerequisite for the preparation of multicompartment micelles is utilization of three different blocks for creation of the micellar aggregate. Whereas anionic polymerization still has its reputation in producing most well-defined block terpolymers or miktoarm star terpolymers, controlled radical polymerization techniques have emerged as a second means for the preparation of sophisticated subdivided colloidal structures. The higher tolerance toward functional groups is the particular benefit of the latter techniques.

Interestingly, in the field of bis-hydrophilic block terpolymers, a dominant interest has so far been placed on preparation of ABC block terpolymers with a hydrophobic A block and two hydrophilic blocks connected to each other (B + C). Typically, these polymers lead to core−shell−corona micelles and were investigated by a variety of groups.[39−46] Surprisingly, preparation of terpolymers with two outer hydrophilic blocks and one inner hydrophobic block has not yet been subjected to intense research.[15,17] Some success has been reported by Eisenberg and Meier, who prepared vesicles with asymmetric walls based on specifically tailored block terpolymers.[47−49] Use of these vesicles as nanocontainers with different internal and external walls was suggested, demonstrating interest in these structures. Moreover, depending on the interaction of the two outer blocks, A and B, mixed and phase-segregated structures within the

* To whom correspondence should be addressed. E-mail: Axel.Mueller@uni-bayreuth.de.
[†] Universität Bayreuth.
[‡] The University of New South Wales.
[§] Current address: Preparative Macromolecular Chemistry, Institut für Technische Chemie and Polymerchemie, Universität Karlsruhe (TH)/ Karlsruhe Institute of Technology (KIT), Engesserstrasse 18, 76128 Karlsruhe, Germany.

10.1021/ma801215q CCC: $40.75
Published on Web 10/31/2008

corona can be anticipated.[50] In the case of the structures with mixed coronas, a facile tunability of the corona is possible by changing the degree of polymerization of the two end blocks. In addition, both blocks can be used for sensing the environment, which is not possible for core−shell−corona structures. Additional modification of the structures is possible via incorporating stimuli-sensitive blocks, and access to different particle architectures is feasible by changing the hydrophilic-to-hydrophobic balance. With these features a large diversity of different multicompartment particles can be imagined and tailored for specific applications. Some results were recently reported concerning creation of similar desired structures using coassembly of two diblocks, either by forcing them into a complex−core coacervate micelle (C3M) or simple undirected comicellization.[51,52] Depending on the corona-forming blocks, C3Ms can undergo phase separation in the corona.[53] However, both approaches have some disadvantages. First, C3Ms are only stable in medium of low salinity, and moreover, structures with high aspect ratios such as cylinders could not yet been achieved. For comicellization of two block copolymers having the same end block, the drawbacks are obvious. Comicellization is only a statistical process, and thus, the micellar structure, in particular the corona composition, cannot be precisely controlled. Some theoretical considerations even suggest that two populations of homogeneous micelles, each just composed of one kind of diblock copolymer mixture, can coexist.[54] Besides, studies so far only included core-forming blocks with high glass-transition temperatures, which hinder structural rearrangements after comicellization and minimize the possibilities of structural rearrangements toward external stimuli.

Herein, we present the synthesis of novel bis-hydrophilic block terpolymers via RAFT polymerization[55−57] as well as results concerning characterization of the solution behavior of the resulting polymers in water with respect to the dynamics of the core-forming block and the particle architecture. Poly(ethylene oxide) (PEO) and various poly(meth)acrylamide derivatives are used as hydrophilic blocks. Poly(meth)acrylamide derivatives exhibit different solution characteristics depending on the substitution pattern at the amide functions. Polyacrylamide (PAAm) without any hydrophobic substitutes is an extremely polar, highly water-soluble polymer, which does not show any lower critical solution temperature (LCST) behavior. It is known to undergo phase separation with PEO, thus leading to Janus micelles.[53] Upon addition of hydrophobic substituents to the amide function, e.g., *N*-(isopropyl)acrylamide (NIPAAm) or *N*,*N*-(diethyl)acrylamide (DEAAm), the polymers PDEAAm and PNIPAAm exhibit an appealing stimuli-responsive LCST behavior with different LCSTs. Poly(*N*-(2-hydroxypropyl)-methacrylamide) (PHPMA) is a nonimmunogenic polymer and has an addressable hydroxyl function which allows conjugation to drugs or units for cell recognition.[58−61] Poly(*n*-butyl acrylate)(PnBuA) serves as an inner hydrophobic block, ensuring high dynamics in the micellar core due to its low glass-transition temperature ($T_g \approx -46$ °C). In terms of synthesis, polymerization of (meth)acrylamides is a domain of radical addition fragmentation transfer (RAFT) polymerization. Therefore, RAFT polymerization was used as it also provides means to assess a library of different block terpolymers in a reasonable time frame. The synthetic strategy first involved preparation of PEO-based macro-chain-transfer agents (macro-CTAs), which were subsequently used for block copolymerization of *n*-butyl acrylate and different (meth)acrylamides. With this approach it is possible to obtain a series of very well defined block terpolymers of different structures. It is shown that the hydrophilic-to-hydrophobic balance can be tuned over a large range and that the ratio of chain lengths of the two outer hydrophilic blocks can be adjusted. In the last section we will highlight some micellar structures to demonstrate the feasibility of the concept and arising possibilities.

Experimental Section

Materials. *N*,*N*-Dimethylformamide (DMF, anhydrous), *N*,*N*-dimethylacetamide (DMAc, anhydrous), 1-methyl-2-pyrrolidinone (NMP, anhydrous), and dimethyl sulfoxide (DMSO, anhydrous) were purchased from Aldrich and used without further purification. Dichloromethane (DCM), diethyl ether, benzene, and ethanol were obtained in p.a. grade and used as received. THF (p.a. grade) was cleaned by distillation from Na/K alloy. *N*,*N*-Azobisisobutyronitrile (AIBN), acrylamide (AAm), and *N*-isopropylacrylamide (NIPAAm) were ordered from Aldrich and recrystallized from ethanol. *N*,*N*-Diethylacrylamide (DEAAm, ABCR chemicals), *N*-(2-hydroxypropyl)methacrylamide (HPMA, ABCR chemicals), monomethoxy poly(ethylene oxide) (M_n = 5000 − PDI = 1.04, M_n = 2000 − PDI = 1.04, Aldrich), 4-(dimethylamino)pyridine (DMAP, Aldrich), dicyclohexylcarbodiimide (DCC, Aldrich), phenylmagnesium bromide solution in diethyl ether 2.8 M (Acros), α-bromophenylacetic acid (Aldrich, 98%), and carbon disulfide (Aldrich, reagent plus >99.9%) were used as received. *N*-Butyl acrylate (nBuA) was purchased from Aldrich in the highest purity available and purified by passing through a basic alumina column.

Polymer Characterization. *SEC in THF.* SEC in THF was conducted at an elution rate of 1 mL·min^{-1} using a Shodex RI-101 detector, a Waters 996 photodiode array detector (PDA), and PSS SDVgel columns (300 × 8 mm, 5 μm): 10^5, 10^4, 10^3, and 10^2 Å. Polystyrene standards were used to calibrate the columns, and toluene was used as an internal standard.

SEC in NMP. Polymers were characterized by size exclusion chromatography (SEC) using a Waters 510 HPLC pump, a Bischoff 8110 RI detector, a Waters 486 UV detector (λ = 270 nm), and a 0.05 M solution of LiBr in 2-*N*-methylpyrrolidone (NMP) as eluent. PSS GRAM columns (300 × 8 mm, 7 μm; 10^3, 10^2 Å (PSS, Mainz, Germany)) were thermostatted at 70 °C. A 20 μL amount of a 0.4 wt % polymer solution was injected at an elution rate of 1 mL·min^{-1}. Polystyrene standards were used to calibrate the columns, and methyl benzoate was used as an internal standard.

SEC in DMAc. For DMAc SEC measurements, dimethylacetamide/0.05% LiBr as the mobile phase (1 mL·min^{-1}), a column set consisted of a PL 5.0 μm bead size guard column and a set of 3 × 5 μm PL linear columns (10^3, 10^4, and 10^5 Å) (70 °C), a DRI detector, and linear polystyrene standards were used.

ESI-MS. Electrospray ionization mass spectrometry experiments were carried out using a Thermo Finnigan LCQ Deca quadrupol ion-trap mass spectrometer (Thermo Finnigan, San Jose, CA) in positive-ion mode. The ESI-MS is equipped with an atmospheric pressure ionization source which operates in the nebulizer-assisted electrospray mode. The instrument was calibrated with caffeine, MRFA, and Ultramark 1621 (all from Aldrich) in the mass range 195−1822 amu. All spectra were acquired over the mass to charge range (*m*/*z*) of 150−2000 Da with a spray voltage of 5 kV, a capillary voltage of 39 V, and a capillary temperature of 275 °C. Nitrogen was used as sheath gas (flow = 40 of maximum), while helium was used as auxiliary gas (flow = 5% of maximum). The solvent was a 6:4 v/v mixture of THF/methanol with a polymer concentration of ∼0.4 mg·mL^{-1}. The instrumental resolution of the employed experimental setup is 0.1 amu. The theoretical isotopic patterns were generated using the Xcalibur program included with the Thermo Finnigan LCQ Deca ion trap mass spectrometer.

Liquid Adsorption Chromatography under Critical Conditions (LACCC). Liquid adsorption chromatography under critical conditions (LACCC) was conducted on a chromatographic system composed of a degasser ERC 3415α, a pump P4000 (TSP), and an autosampler AS3000 (TSP). Two detectors were used: a UV detector UV6000LP (TSP) with two wavelengths (λ = 230 and 261 nm) and an evaporative light scattering detector (ELSD) EMD

960 (Polymer Laboratories) operating at 80 °C with a gas flow rate of 6.8 L/min. Two reversed phase columns C18, 250 × 4.6 mm i.d., with 5 μm average particle size were employed, one with 120 Å (YMC) and the other with 300 Å pore diameters (Macherey-Nagel). The solvents, acetonitrile (ACN) and water (H_2O), were HPLC grade and used freshly. The critical solvent composition for polyethylene glycol monomethyl ether (PEO-OH) determined for this system was ACN/H_2O 39.1/60.9 (v/v) at 23 °C with a flow rate of 0.5 mL/min.

Samples were dissolved in the critical mix at a concentration of 0.2 wt %. Then 20 μL was injected. Modified PEO-OH appeared in adsorption mode due to the low polarity of the end group. To obtain a narrow and well-defined peak, a gradient was used after the elution time of remaining PEO-OH. The composition sequence is detailed here. The critical composition was maintained for 16 min. Then, over 16 min, a linear gradient up to 60% of ACN was realized. This percentage was decreased directly to the critical composition over 1 min also with a linear gradient. Finally, this proportion was kept for 60 min to equilibrate the system before the next measurement.

MALDI-ToF-MS. Matrix-assisted laser desorption time of flight mass spectra were recorded on a Bruker Reflex III operated in linear mode using a nitrogen laser (337 nm) and an accelerating voltage of 20 kV. 2,5-Dihydroxybenzoic acid, 2,4,6-trihydroxyacetophenone monohydrate, *trans*-2-[3,4-*tert*-butylphenyl-2-methyl-2-propenyliden-]malononitrile, 3-indoleacrylic acid, 2′-(4-hydroxyphenylazo) benzoic acid, or dithranol was used as matrix. Samples were prepared from DMAc or DMSO solution by mixing matrix (20 mg·mL^{-1}) and sample (10 mg·mL^{-1}) in a ratio 4:1 or mixing matrix (20 mg·mL^{-1}), sample (10 mg·mL^{-1}), and salt (sodium trifluoracetate or potassium trifluoracetate, 10 mg·mL^{-1}) in a ratio of 20:5:1.

NMR. ^{1}H and ^{13}C NMR spectra were recorded on a Bruker AC-250 spectrometer in various solvents at room temperature. The 2D-HMBC spectrum of PEO-2k-CTA was acquired on a Bruker Avance 300.

Synthesis. *α-Bromophenylacetate-Terminated Poly(ethylene oxide) (PEO-Br).* A 10 g amount of PEO (M_n = 5000, 2 mmol) was dissolved in 50 mL of DCM. Afterward, DMAP (49 mg, 0.4 mmol), DCC (2.07 g, 10 mmol), and α-bromophenylacetic acid (1.29 g, 6 mmol) were added, and the solution was stirred for 24 h at room temperature under nitrogen atmosphere. After filtration, the product was precipitated into cold diethyl ether. Further purification was accomplished by several cycles of product redissolution in warm ethanol, precipitation at low temperatures, and subsequent centrifugation. Finally, the functionalized PEO derivative was dialyzed against benzene and freeze dried with a final yield of around 80−90%. NMR characterization is provided in the Supporting Information and elsewhere.[62]

Synthesis of PEO Macro-Chain-Transfer Agents (PEO-CTA). A 10 g amount of freeze-dried PEO-Br was heated to 60 °C in high vacuum overnight. Subsequently, 50 mL of anhydrous THF was added under a nitrogen flow, and a clear solution was obtained by slight heating. In a second reaction flask, carbon disulfide (0.26 mL, 4.4 mmol) was added with a syringe to a degassed THF solution (10 mL) of phenylmagnesium bromide (1.43 mL of 2.8 M solution in diethyl ether, 4 mmol). This flask was allowed to stand at room temperature for 30 min and then heated to 50 °C for another 30 min. Afterward, the dark-red solution was transferred with a syringe to an addition funnel connected to the flask containing the PEO-Br solution in degassed THF. The solution was added dropwise at room temperature, and the reaction was allowed to proceed for 3 h. After precipitation into cold hexane, the product, PEO-CTA, was purified in the same way as PEO-Br with a final yield of 80−90%. NMR characterization is provided in the Supporting Information and elsewhere.[62]

PEO-block-PnBuA Diblock Copolymers. A representative example is as follows. A mixture of PEO-5k-CTA (0.3 g, 0.06 mmol), nBuA (5.76 g, 45 mmol), and DMF (3.29 g, 45 mmol) in a screw-cap flask, sealed with a rubber septum, was degassed by bubbling with nitrogen. In a second flask, a stock solution of AIBN (19.7 mg, 0.12 mmol) in DMF (10 mL) was degassed similarly. Afterward, 1 mL of this stock solution was transferred to the reaction mixture with a syringe and the polymerization flask was placed into an oil bath at 60 °C. Samples were withdrawn to monitor conversion and obtain PEO-*block*-PnBuA diblock copolymers of desired compositions. The polymer was isolated from the samples via dilution with ethanol (rapid cooling) and subsequently dialyzed against benzene to remove residual solvent and monomer. Freeze drying of the samples yielded the final pure diblock copolymers in near quantitative yields. NMR characterization is provided in the Supporting Information.

PEO-block-PnBuA-block-PNIPAAm, PEO-block-PnBuA-block-PDEAAm, and PEO-block-PnBuA-block-PHPMA Block Terpolymers. All block terpolymers having PNIPAAm, PDEAAm, or PHPMA end blocks can be synthesized in an analogous fashion. In the case of DEAAm (liquid monomer), only 50% of solvent of the following representative experiment was added. A representative example for PEO-*block*-PnBuA-*block*-PNIPAAm is as follows. A 1 g amount of PEO-*block*-PnBuA ($M_{n,calcd}$ = 18 700, 0.054 mmol) was dissolved in DMF (6.46 g, 88 mmol). After complete dissolution, NIPAAm (5 g, 44 mmol) was added and the mixture was degassed by bubbling with nitrogen. Subsequently, 0.5 mL of a degassed stock solution of AIBN (63.7 mg, 0.388 mmol) in 10 mL of DMSO was introduced into the reaction mixture and the flask was placed into an oil bath thermostatted at 60 °C. Samples were withdrawn to monitor conversion and obtain block terpolymers of desired compositions. The polymer was isolated from the samples via dilution with dioxane or DMSO (rapid cooling) and subsequently dialyzed against dioxane or water (for PHPMA-based triblock copolymers) to remove residual solvent and monomer. Freeze drying of the samples yielded the final pure triblock copolymers in near quantitative yields. NMR characterization is provided in the Supporting Information.

PEO-block-PnBuA-block-PAAm. All polymerizations were conducted in a mixed solvent system of DMF and DMSO. DMF is used to initially dissolve the PEO-*block*-PnBuA diblock copolymers, which do not readily dissolve in DMSO. DMSO is needed as solvent for polymerization due to the solubility characteristics of PAAm. In a typical experiment, 1 g of PEO-*block*-PnBuA ($M_{n,calcd}$ = 37 000, 0.0272 mmol) was dissolved in 2 g of DMF. Subsequently, 3 mL of DMSO and 1.1 g of AAm (15.5 mmol) were added to this flask and the solution was deoxygenated by bubbling with nitrogen. Subsequently, 0.5 mL of a degassed stock solution of AIBN (8.9 mg, 0.054 mmol) in 5 mL of DMSO was introduced into the reaction mixture and the flask was placed into an oil bath thermostatted at 60 °C. Samples were withdrawn to monitor conversion and obtain block terpolymers of desired compositions. The polymer was isolated from the samples via dilution with DMSO (rapid cooling) and subsequently dialyzed against water to remove residual solvent and monomer. Freeze drying of the samples yielded the final pure block terpolymers in near quantitative yields. NMR characterization is provided in the Supporting Information.

Solution Characterization of Aggregates. *Formation of Aggregates.* Micelles were prepared by dissolution of the polymers (c = 5 mg·mL^{-1}) in water at room temperature and prolonged stirring. In case of dialysis, the polymer solution in dioxane or DMSO (5 mg·mL^{-1}) was exchanged stepwise to water in a dialysis cell using dialysis membranes with a MWCO of 5000−10000 kDa.

For cryogenic transmission electron microscopy (cryo-TEM) studies a drop of the sample dissolved in water was put on a lacey transmission electron microscopy (TEM) grid, where most of the liquid was removed with blotting paper, leaving a thin film stretched over the lace. The specimens were instantly vitrified by rapid immersion into liquid ethane and cooled to approximately 90 K by liquid nitrogen in a temperature-controlled freezing unit (Zeiss Cryobox, Zeiss NTS GmbH, Oberkochen, Germany). The temperature was monitored and kept constant in the chamber during all of the sample preparation steps. After freezing the specimens, the specimen was inserted into a cryo-transfer holder (CT3500, Gatan, München, Germany) and transferred to a Zeiss EM922 EF-TEM instrument. Examinations were carried out at temperatures around 90 K. The transmission electron microscope was operated at an

Scheme 1. Synthetic Access to PEO-Based Macro-Chain-Transfer Agents (PEO-CTAs)

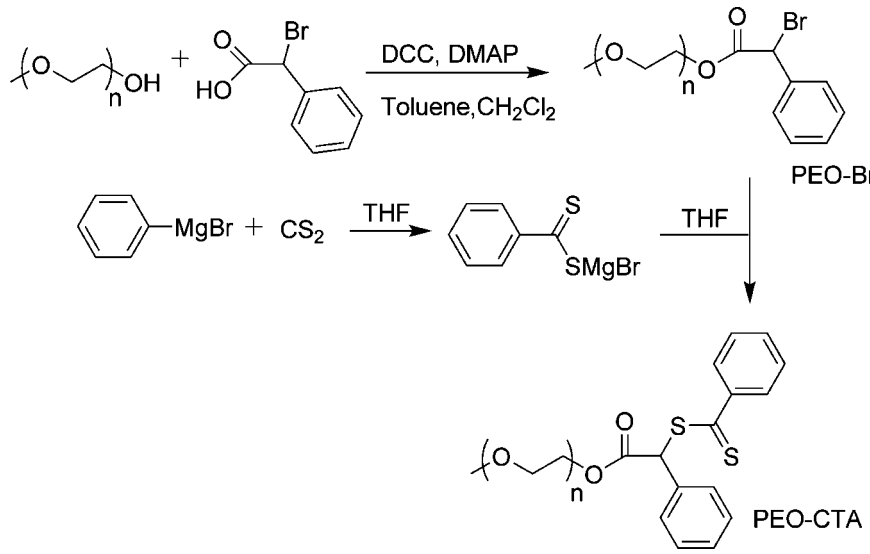

acceleration voltage of 200 kV. Zero-loss filtered images ($\Delta E = 0$ eV) were taken under reduced dose conditions. All images were registered digitally by a bottom-mounted CCD camera system (Ultrascan 1000, Gatan) combined and processed with a digital imaging processing system (Gatan Digital Micrograph 3.9 for GMS 1.4).

Dynamic Light Scattering (DLS). Dynamic light scattering was performed on an ALV DLS/SLS-SP 5022F compact goniometer system with an ALV 5000/E cross-correlator and a He−Ne laser ($\lambda_0 = 632.8$ nm). An automatic thermostatting control system was used for the temperature sweeps. The heating steps were chosen to either 1 or 2 K. Prior to each measurement, the sample was allowed to equilibrate for 10 min. Data evaluation of the dynamic light scattering measurements was performed with the CONTIN algorithm.

Results and Discussion

Synthesis and Characterization of PEO-CTA. The most important prerequisite for the successful synthesis of block copolymers via RAFT using a macro-chain-transfer agent (CTA) is the near quantitative coupling of the first block to the CTA.[63] Otherwise, a significant fraction of the first unmodified block contaminates the final block copolymers. Synthetic access toward poly(ethylene oxide)-based CTAs is outlined in Scheme 1 and was adapted similarly from Hawker and co-workers.[62] PEO-CTAs of this kind have not yet widely been used for RAFT polymerization.[64] Herein, two poly(ethylene oxides) of different molecular weights ($M_n = 2000$ g·mol^{-1}= PEO-2k and $M_n = 5000$ g·mol^{-1} = PEO-5k) were used.

Due to the necessity of ensuring sufficient conversion of the hydroxyl group of the PEO-OH, various techniques were used for analysis. Product formation was monitored using NMR, ESI-MS (electrospray ionization mass spectrometry), and LACCC (liquid adsorption chromatography at critical conditions). The structure of PEO-2k-Br and the connection of the CTA moiety to the PEO chain within PEO-2k-CTA can be confirmed with a straightforward assignment of the peaks in the ^{1}H, ^{13}C, and a 2D-HMBC spectra (Supporting Information). A comparison of the signals of PEO and the CTA group indicates a near quantitative formation of the desired product. However, estimation of the extent of end-group functionalization based on ^{1}H NMR loses reliability for higher degrees of polymerization (DP) of PEO, i.e., for PEO-5k-CTA having a DP of 114. Successful formation of the product and intermediate was furthermore confirmed by ESI-MS, as shown in Figure 1.[65] The isotopic patterns found correspond well to the simulated one of the target compounds. Some minor peaks can found for PEO-2k-Br and PEO-2k-CTA. In the case of PEO-2k-CTA, one minor peak pattern can be assigned to a K species, induced by ionization of the compound with potassium, or PEO-2k-OH (1793−1796 amu). The other peaks may be caused by minor synthetic byproducts with good ionization capabilities or degradation processes during the ESI process or sample preparation[66] as they cannot be assigned with any charged species of neither PEO-OH nor PEO-Br.

After qualitative confirmation of the product structure by means of NMR and ESI-MS, LACCC was used to quantitatively analyze the end-group modification starting from PEO-OH. LACCC is one of the only techniques that is exclusively sensitive to modifications of the end group of a polymer molecule when keeping the side groups or repeating units

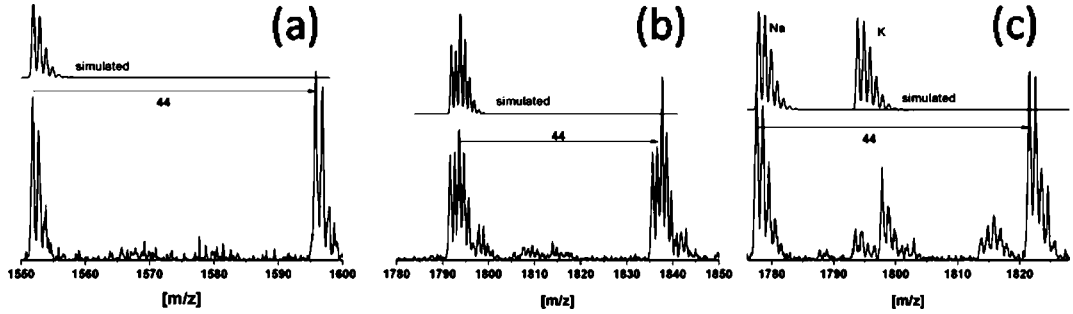

Figure 1. ESI-MS of PEO-2k-OH (a), PEO-2k-Br (b), and PEO-2k-CTA (c). Simulated spectra of the target compounds are shown for comparison (Na species for b and c, K species for c).

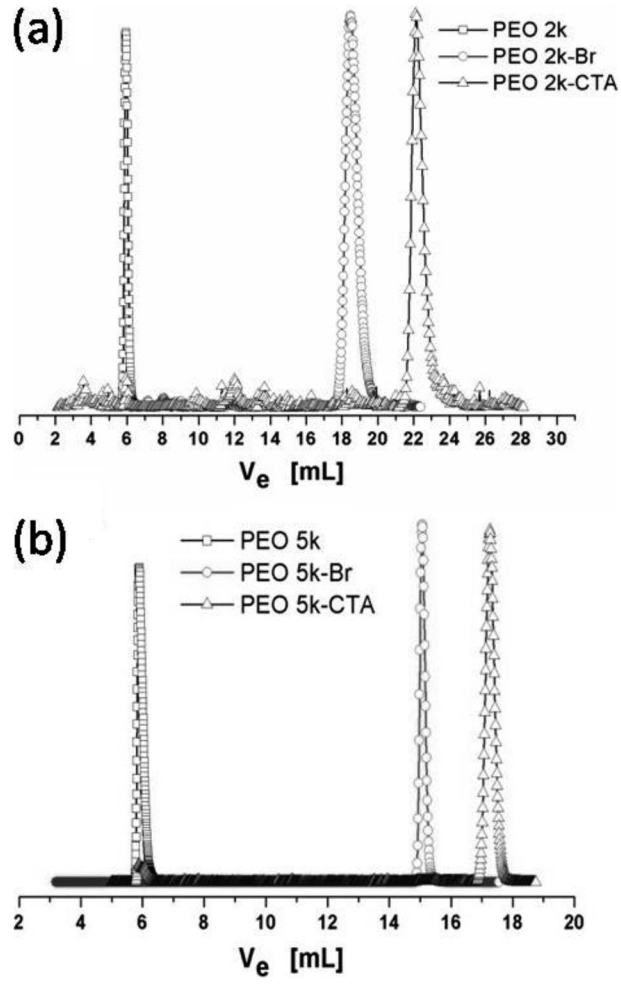

Figure 2. LACCC traces of various end-group-modified PEOs as indicated in the graphs. A solvent gradient was applied after a certain time in order to force elution of PEO-Br and PEO-CTA and minimize the measurement time.

unreacted. For these conditions, adsorption of the monomer units (HPLC mode) and separation by the hydrodynamic volume (SEC mode) are exactly balanced and any change in the elution volume solely arises from chemical changes of the end group. LACCC can be applied for a wide range of molecular weights and is the technique of choice for quantitative assessment of the extent of functionalization of the end groups. Figure 2 displays the LACCC traces for all steps of the functionalization and both molecular weights of the PEO. For both chain lengths of PEO modification with the α-bromophenylacetic acid proceeds quantitatively as can be seen from the full shift of the traces for PEO-OH (squares) to PEO-Br (circles). After careful optimization of the reaction from PEO-Br to PEO-CTA (triangles), this reaction is also almost fully quantitative. A slight cleavage of the initially formed ester function can be observed, leading to reappearance of tiny peaks at the elution volume of PEO-OH. A small peak corresponding to the released PEO-OH can also be found in the ESI-MS data of PEO-2k-CTA (1793−1796 amu). This cleavage process was a major side reaction which needed to be suppressed during optimization of the reaction conditions. It was accomplished by reducing the reaction time and temperature to 3 h at room temperature under our conditions. Refluxing for prolonged time was not necessary; on the contrary, it led to an amplification of the cleavage process. Further significant side products cannot be observed, which also confirms the additional peaks in the ESI-MS data to be mostly irrelevant for the following polymerizations.

In conclusion, several analytical methods have been used to confirm the near quantitative preparation of PEO-based macro-CTAs of different molecular weights. The developed reaction conditions allow the fast and straightforward preparation of pure PEO-CTAs.

Synthesis and Characterization of PEO-*block*-PnBuA Diblock Copolymers. *N*-Butyl acrylate (n-BuA) was chosen for polymerization of the second block because of its low glass-transition temperature. The low glass-transition temperature facilitates the dynamic behavior of micelles in water. A hydrophobic block with a high glass-transition temperature, e.g., poly(methyl methacrylate), polystyrene, or poly(vinylpyridine), would lead to so-called frozen micelles and limit a responsive behavior.

The polymerization kinetics for *n*-BuA using both PEO-CTAs are shown in Figure 3. Note that all plots are composed of at least two reactions, demonstrating a very high reproducibility of the reactions. For both molecular weights of PEO-CTA, linear time conversion plots, being indicative for a constant radical concentration, and an almost linear increase of the molecular weight with conversion can be observed, indicating a well-controlled RAFT process taking place. The deviation from exact linearity of the evolution of molecular weights in dependence of the conversion can be understood considering the different hydrodynamic dimensions as a function of the composition and non-absolute calibration of the SEC system. The polydispersity indices remain very low (PDI < 1.1) within the investigated conversion range. The SEC elution traces show an onset of interchain coupling for conversions higher than 20%. These expected[67] but nevertheless unwanted termination reactions show the necessity of stopping the reactions at a moderately low conversion of 20−25%. Only under these circumstances, block copolymers are obtained which still carry the RAFT end group to a major extent and allow sufficient block extension toward block terpolymers.

Strikingly, since great efforts were made to obtain quantitatively functionalized PEO-CTAs, almost no residual precursor can be found contaminating the diblock copolymers. The blocking efficiency is very high, and a separation of residual homopolymer from the diblock copolymer is not necessary as it was in some other studies.[64] Table 1 summarizes the various polymers synthesized following the considerations mentioned above.

Independent of the PEO-CTA used, various degrees of polymerizations can be obtained for the second block, demonstrating the versatility of our approach. If the target is a very long second block, the monomer feed can easily be increased without losing control of the reaction or leading to unreasonably long reaction times. The experimentally determined values using SEC with a PS calibration curve only give apparent molecular weights. The calculated values were confirmed in several cases by MALDI-ToF measurements of some diblock copolymers which show a satisfying agreement (Supporting Information).

In conclusion, RAFT polymerization of *n*-BuA in conjunction with highly functionalized PEO-CTAs provides very well defined PEO-*block*-PnBuA diblock copolymers with tailored block ratios. Separation of homopolymer and diblock copolymer is unnecessary. Additionally, high molecular weights are accessible without the appearance of significant termination reactions. A key step toward synthesis of the desired bis-hydrophilic block terpolymers is based on limiting conversion in order to obtain diblock copolymers with a high degree of CTA groups attached to their chain ends.

Synthesis and Characterization of Bis-Hydrophilic Block Terpolymers. Various (meth)acrylamide derivatives were chosen for polymerization of the third block in order to obtain bis-hydrophilic terpolymers with two hydrophilic end blocks. In

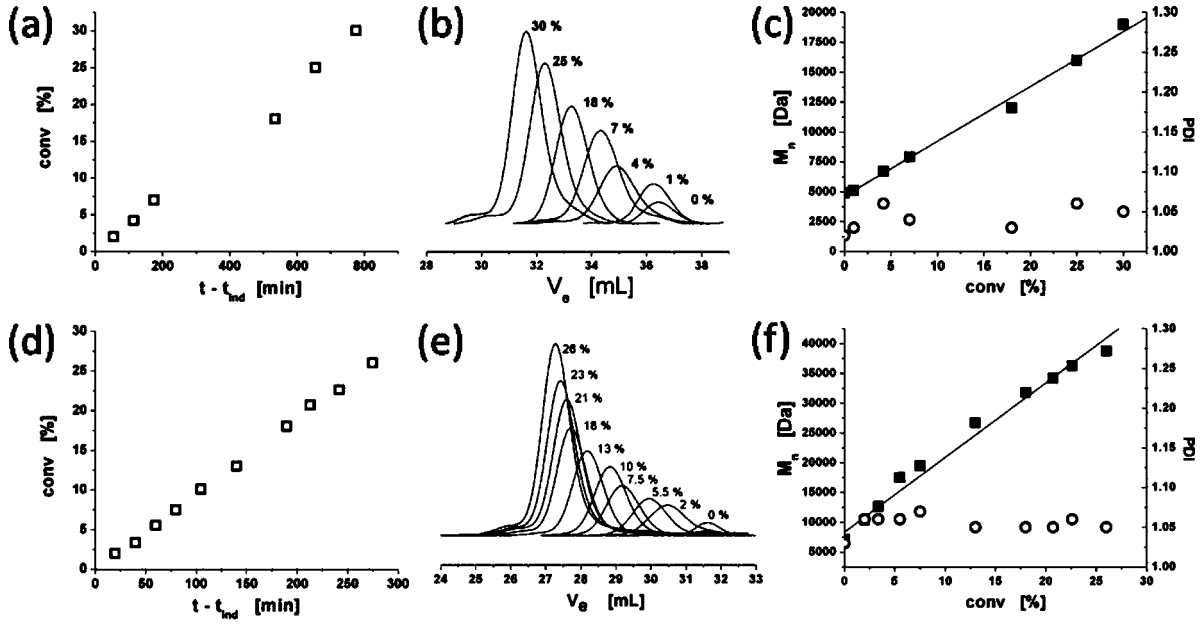

Figure 3. Results for polymerization of *n*-BuA using PEO-2k-CTA (top, a−c) and PEO-5k-CTA (bottom, d−f). Time conversion plots (a and d), SEC elution traces (b and e), and evolution of molecular weights and polydispersity indices as a function of conversion. The induction period[68] (30 min) was subtracted for the time conversion plots to allow a better display of the data points.

Table 1. Overview of PEO-*block*-PnBuA Diblock Copolymers

diblock copolymers[a]	$M_{n,SEC}$[b] (PDI)	$M_{n,calcd}$[c]	$M_{n,MALDI}$
PEO45-PnBuA29	7700 (1.07)	6000	6100 (1.13)
PEO45-PnBuA100	18 500 (1.07)	18 200	17 400 (1.09)
PEO114-PnBuA105	20 600 (1.05)	18 700	16 900 (1.11)
PEO114-PnBuA201	31 800 (1.05)	31 000	
PEO114-PnBuA250	37 300 (1.09)	37 200	36 500 (1.09)
PEO114-PnBuA778	82 200 (1.08)	105 000	

[a] The numbers behind the individual blocks correspond to the degree of polymerization, as determined by ^{1}H NMR. [b] SEC in THF calibrated with PS standards. [c] Calculation based on the weight fractions determined by ^{1}H NMR and the true molecular weight of the PEO-CTA.

general, (meth)acrylamides are a very versatile class of monomer as they exhibit different solution behavior depending on the substitution pattern used. A main focus for polymerization toward block terpolymers was set on the PEO-5k-CTA-based block copolymers as longer polymer chains lead to larger sizes of their micellar aggregates and thus facilitate later investigations with cryo-TEM. Furthermore, the tendency for two polymers to phase segregate scales with their number of repeating units, which obviously increases for higher chain lengths of PEO. Nevertheless, one run was conducted for the shorter PEO based block copolymers to convincingly demonstrate the good control over the reaction parameters. For analysis of the block terpolymers one has to distinguish between two sets of terpolymers: The first group consists of PEO-*block*-PnBuA-*block*-PDEAAm and PEO-*block*-PnBuA-*block*-PNIPAAm copolymers which both carry thermo-responsive segments of moderate polarity. These block terpolymers can be analyzed in a rather straightforward manner. The second set comprises PEO-*block*-PnBuA-*block*-PHPMA and PEO-*block*-PnBuA-*block*-PAAm block terpolymers. Those carry permanently water-soluble end blocks of very high polarity. Their extremely limited solubility in the unimolecular, nonassociated form remains a challenging aspect in their characterization as will be pointed out below. Nevertheless, both polymers are very interesting as the PEO/PAAm system has a high tendency to phase segregate and PEO/PHPMA is very interesting in terms of biomedical applications.

Considering the first group, the kinetic data of several runs for preparation of PEO-*block*-PnBuA-*block*-PDEAAm and PEO-*block*-PnBuA-*block*-PNIPAAm are shown in Figure 4. All polymerizations show characteristics of a controlled chain-transfer reaction taking place. The time conversion plots are linear, and there is a linear increase of molecular weight with increasing conversion. Extension of the third block can be performed independently of the PEO chain length as can be seen by comparing the two top rows, which list data for PEO-2k- and PEO-5k-based block terpolymers. Under similar conditions, polymerization of DEAAm is almost five times faster than compared to NIPAAm, yet still exhibiting a high level of control. Whereas a significant recombination shoulder occurs around 20−25% conversion in the case of PEO-*block*-PnBuA-*block*-PNIPAAm block terpolymers, it is absent for all PEO-*block*-PnBuA-*block*-PDEAAm polymers until a conversion of up to 40%. All SEC elution traces show a distinct shift toward shorter elution volumes with increasing conversion. The whole peak is displaced, indicating an almost complete blocking efficiency from the second to the third block. These good results obviously benefit from the fact that polymerizations of the diblock copolymers, PEO-*block*-PnBuA, had been stopped at low conversions, ensuring a high extent of capping with the CTA. Note that the PEO-*block*-PnBuA-*block*-PDEAAm block terpolymers can also be analyzed with a standard THF SEC, whereas more polar eluents, such as NMP, are required for PEO-*block*-PnBuA-*block*-PNIPAAm.

The most well-defined block terpolymers can again be obtained by limiting conversion to a moderate degree, depending on the monomer used. For micellization studies suppression of interchain coupling, leading to ABCCBA structures, is important as this could lead to intermicellar connections and flower-like micelles. The compositions of all block terpolymers, including the second group of PEO-*block*-PnBuA-*block*-PHPMA and PEO-*block*-PnBuA-*block*-PAAm, were confirmed by ^{1}H NMR. The spectra including the peak assignments are shown in the Supporting Information, confirming the compositions of all block terpolymers. Due to the moderate speed and viscosity of the polymerizations, samples can easily be taken at various points to obtain block terpolymers with varying degrees of polymerization for the end block. This sampling allows a final tuning of the corona structure of the resulting micelles. To keep sufficient clarity, Table 2 only displays the final polymers (last samples) at high degrees of polymerization for the last block

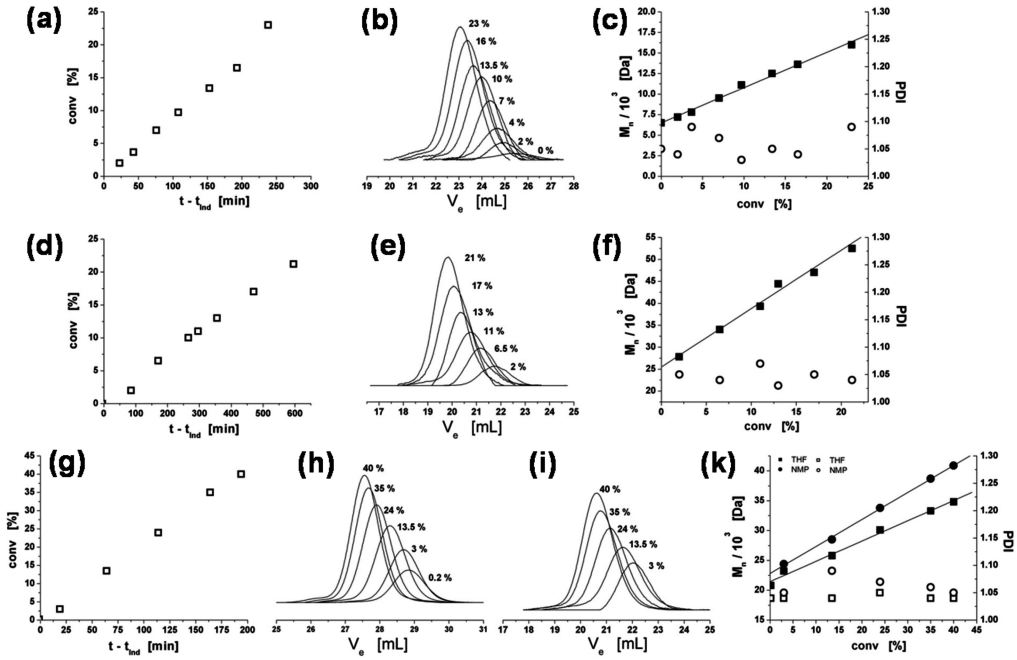

Figure 4. Time conversion plots (a, d, g), SEC elution traces (b, e, h, i), and evolution of molecular weights and polydispersities as a function of conversion (c, f, k) for the block extension of PEO45-PnBuA29 with NIPAAM (a−c) and PEO114-PnBuA105 with NIPAAm (d−f) and DEAAM (g−h). For DEAAM, both THF (h) and NMP (i) SEC traces and analysis are shown. The induction period[68] (20−25 min) was subtracted for the time conversion plots to allow a better display of the data points.

Table 2. Overview of the Block Terpolymers Synthesized

block terpolymer[a]	$M_{n,SEC}$ (PDI)[b]	$M_{n,calcd}$[d]	$M_{n,MALDI}$ (PDI)
PEO114-PnBuA105-PDEAAm181	34 800 (1.04) 40 900 (1.05)[c]	41 800	42 700 (1.02)
PEO114-PnBuA250-PDEAAm200	54 000 (1.06) 60 500 (1.07)[c]	62 600	69 000 (1.02)
(PEO114-PnBuA250-PDEAAm99)	(46 600 (1.06))	(49 800)	(48 400 (1.03))
PEO45-PnBuA29-PNIPAAm46	15 900 (1.10)	11 200	12 600 (1.03)
PEO114-PnBuA105-PNIPAAm350	66 200 (1.09)	58 250	n.a.
(PEO114-PnBuA105-PNIPAAm275)	(56 000 (1.12))	(49 800)	(48 400 (1.04))
(PEO114-PnBuA105-PNIPAAm195)	(52 500 (1.04))	(40 700)	(43 500 (1.03))
PEO114-PnBuA250-PNIPAAm217	70 000 (1.05)	61 700	
(PEO114-PnBuA250-PNIPAAm82)	(51 800 (1.05))	(46 500)	(45 928 (1.03))
PEO114-PnBuA105-PAAm195	−	30 900	−
PEO114-PnBuA250-PAAm120	−	48 200	−
PEO114-PnBuA105-PHPMA129	−	36 700	−
PEO114-PnBuA250-PHPMA93	−	50 300	−

[a] The numbers behind the individual blocks correspond to the degree of polymerization, as determined by ^{1}H NMR [b] SEC was performed in NMP using a PS calibration curve. [c] SEC was performed in THF using a PS calibration curve. [d] Calculation based on the weight fractions determined by ^{1}H NMR and the true molecular weight of the PEO-CTA.

and for some intermediate samples which were used for MALDI-ToF characterization. Note that MALDI-ToF analysis of amphiphilic block terpolymers is a challenging task. Due to the significantly different solubility characteristics, the polymers tend to form physical aggregates in a wide variety of solvents. Nevertheless, we were able to obtain several meaningful MALDI-ToF spectra for some selected PEO-*block*-PnBuA-*block*-PDEAAm and PEO-*block*-PnBuA-*block*-PNIPAAm polymers (Supporting Information). The MALDI-ToF data coincides well with the calculated molecular weights of the various polymers and convincingly demonstrates the successful and controlled extension. Consequently, the block terpolymers can be tailored in their composition and molecular weights over a wide range.

The situation regarding analysis of the second set of terpolymers, utilizing the very polar monomers HPMA and AAm, is different. Due to the presence of the extremely polar segments as end blocks, the solubility characteristics are altered in a very undesirable fashion. Even in solvents with a high solvating power, such as DMAc, DMF, NMP, and DMSO, the polymers form aggregates or do not dissolve sufficiently, thus strongly complicating analytical techniques such as SEC or MALDI-ToF. The kinetic data and SEC results are shown in Figure 5. Both polymerizations of HMPA (Figure 5b) and AAm (Figure 5a) show a linear behavior in the time conversion plot, indicating a controlled chain-transfer reaction at a constant radical concentration taking place. In contrast to the block extension with HPMA, which exhibits a strictly linear behavior, all polymerizations with AAm show a decrease of the reaction rate at conversions exceeding 20%. Such a behavior can be correlated with discoloration of the reaction solution from pink to orange for conversions higher than 20%, indicating an undesirable side reaction of the CTA. Most probably, the amide groups of the AAm undergo some side reactions with the dithioester function of the CTA moiety, leading to a decrease in the reaction rate. Consequently, conversion shall be limited to values lower than 20% to minimize this effect and obtain the most well-defined polymers of this type possible. A limited broadening of the molecular weight distribution cannot be excluded at higher conversions. Likewise, since HPMA is a methacrylamide

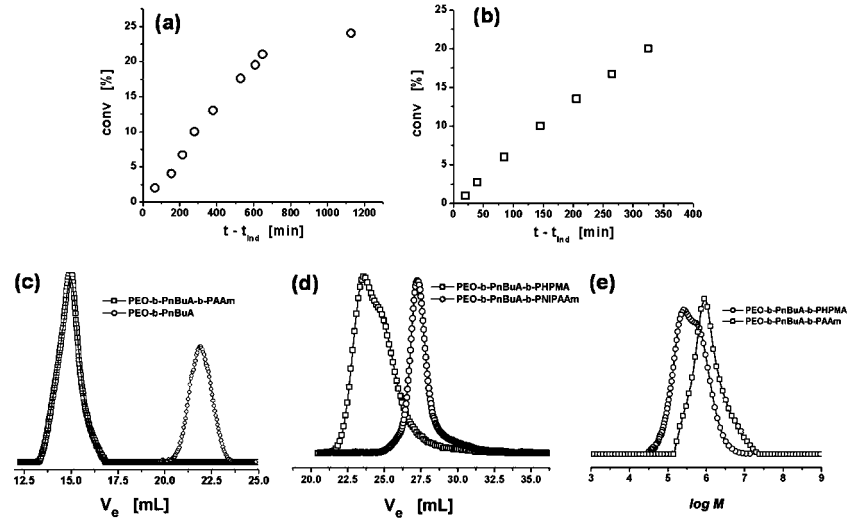

Figure 5. Typical time conversion plots for the block extension of PEO-*block*-PnBuA diblock copolymers with AAm (a) and HPMA (b). The induction periods[68] (160 and 95 min) were subtracted for the time conversion plots to allow a better display of the data points. (c) NMP SEC elution traces of the PEO-*block*-PnBuA diblock copolymer precursor and aggregates formed after block extension with AAm, as indicated in the graph. (d) DMAc SEC elution traces of the aggregates formed by PEO-*block*-PnBuA-*block*-PHPMA polymers. The elution trace of a PEO-*block*-PnBuA-*block*-PNIPAAm of similar degrees of polymerization for each block is shown for comparison. (e) Molecular weight distribution profiles for the PEO-*block*-PnBuA-*block*-PHPMA and PEO-*block*-PnBuA-*block*-PAAm triblock copolymers shown in d and c.

derivative, which is used for chain extension of an acrylate chain end, some increase in the polydispersity index can be anticipated.

Nevertheless, a controlled chain extension taking place is strongly indicated by the (i) continuous change in solubility of the various isolated block terpolymers with different chain lengths of the third block (see Supporting Information for comments), (ii) SEC results showing the absence of any diblock precursor, and (iii) appearance of different aggregate structures of the block terpolymers in water.

Particularly, the SEC data can be used to prove a high blocking efficiency. Both PHPMA- and PAAm-based block terpolymers do even not dissolve readily at room temperature in NMP or DMAc; some heating is always required. The PAAm-based block copolymers do even not dissolve in DMAc at elevated temperatures. Once dissolved at higher temperatures, SEC measurements in NMP and DMAc were conducted for several of those block terpolymers. The behavior is similar for all chain lengths of the third block. A peak corresponding to unimolecularly dissolved polymer molecules cannot be found, not even for the shortest chains of PAAm and PHPMA. The limited solubility of the end blocks in these solvents, as indicated by the temperature required for their dissolution, induces aggregate or micelle formation upon cooling. Consequently, the elution peak appears close to the exclusion volume, resulting in unreasonably high molecular weights. Strikingly and most important for concluding a high blocking efficiency and successful chain extension is the absence of a peak corresponding to residual diblock copolymer, PEO-*block*-PnBuA. The diblock copolymer would not take part in aggregate formation and would lead to peaks at much higher elution volumes as found here. For instance, for the SEC trace in NMP, the corresponding diblock elution trace is shown as comparison (Figure 5c). Similarly, for the DMAc SEC measurements (Figure 5d) the elution trace of a PEO-*block*-PnBuA-*block*-PNIPAAm terpolymer with almost the same degrees of polymerization is shown as an indication for where the PEO-*block*-PnBuA-*block*-PHPMA polymer would be expected. In the case of the block terpolymer, the signal is completely flat, proving the absence of significant amounts of the PEO-*block*-PnBuA diblock precursor. Furthermore, unimolecularly dissolved polymers cannot be found. Note that polymer purification was accomplished via dialysis, and thus, removal of any diblock precursor by selective precipitation is excluded. Additionally, calculation of the theoretical block length of the third block, based on the apparent molecular weight of the SEC measurements (10^5-10^7 Da, Figure 5e), led to extremely high degrees of polymerizations for the third block, which by no means coincides with the fraction determined by ^{1}H NMR. If the molecular weight estimation of the SEC measurements were correct, the blocking efficiency would be significantly below 10% and thus a signal of the residual diblock copolymer precursor would be strongly visible. Since this is not the case, the only explanation is the presence of micellar aggregates during the SEC measurements. The strong aggregation tendency unfortunately prevents using MALDI-ToF, static light scattering, or osmometry for determination of the true molecular weights.

In conclusion, the difficult solubility characteristics prevent in-depth characterization of the second group of block terpolymers in the unimolecular state. However, the kinetic data in combination with the solubility behavior and SEC results, revealing the presence of aggregates and a high blocking efficiency, strongly indicate a successful chain-transfer reaction with controlled increase of molecular weight taking place.

Colloidal Aggregates. Although a full coverage of the complex thermo-responsive behavior and the issue of corona phase segregation is beyond the scope of this report, we nevertheless want to demonstrate the viability of the approach in terms of tuning the aggregate morphology, micellar dynamics, and solution behavior.

On the basis of the selection of PnBuA as hydrophobic block, possessing a low glass-transition temperature far below room temperature, a dynamic behavior of the micelles is expected. Initially, attention was drawn to the dissolution behavior of the block terpolymers. Generally, all polymers do not dissolve instantaneously in water. Depending on the block length and type of the third block, several weeks are required to obtain turbid solutions which do not show any larger particles. The turbidity decreases to some extent during the weeks, indicating dissolution of initially present very large aggregates into smaller ones. Since dissolution times of weeks are not time efficient, the second most common way of preparing micellar solutions via dialysis from a common solvent into a selective solvent, water, was additionally explored.

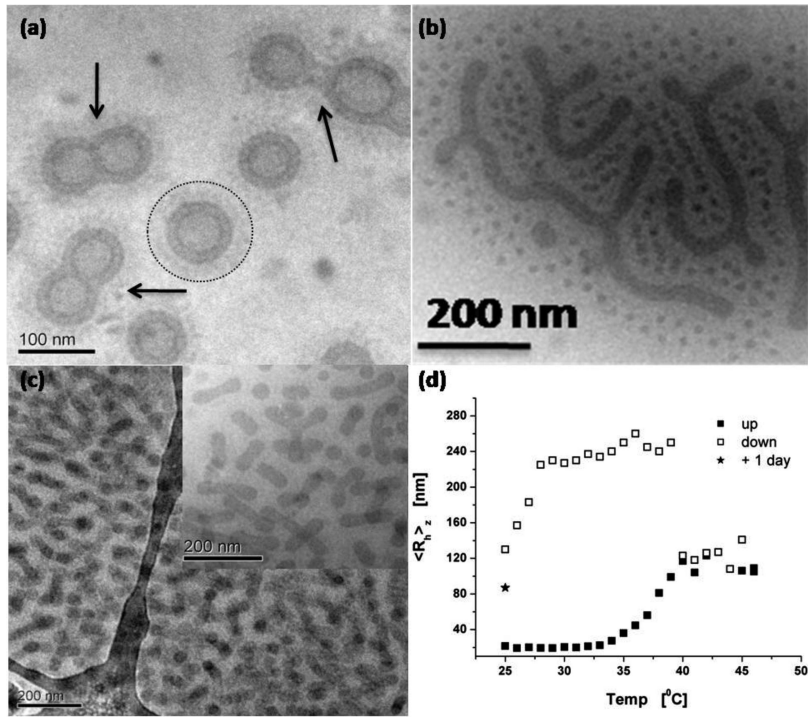

Figure 6. Cryo-TEM images of aggregates formed by PEO114-PnBuA250-PDEAAm135 after direct dissolution in water and stirring for 4 weeks (a), dialysis from dioxane into water (b), and a subsequent heating cycle of the aggregates to 45 °C (c). Temperature-dependent DLS measurement of the spherical micelles in b, obtained by filtration (220 nm pore size). The star indicates an aging time of 1 day.

Some representative cryo-TEM images for a PEO-*block*-PnBuA-*block*-PDEAAm terpolymer with a comparably long hydrophobic block are shown in Figure 6. This example nicely demonstrates the complex and kinetically governed dissolution behavior of the polymers.

Direct dissolution of this polymer into water leads to a large fraction of vesicles (shown in Figure 6a) and a small fraction of branched wormlike aggregates (not shown here). The image shows vesicles surrounded by a corona of PEO or PDEAAm. Several fission processes of vesicles can be seen in the image, which coincide with the observed decrease of turbidity during the weeks of dissolution. On the contrary, dialysis from dioxane into water leads to fractions of smaller and larger spherical micelles and wormlike aggregates (Figure 6b). Thus, direct dissolution favors generation of aggregates of lower curvature. The appearance of several different morphologies depending on the preparation conditions used indicates a strong influence of the kinetics of aggregate formation. The equilibrium state is not reached easily, a phenomenon known for block copolymer-based aggregates.[69−71] A subsequent heating cycle of the latter solution to 45 °C and back to room temperature, hence above the LCST of the PDEAAm, induces a disappearance of the small micelles and a transition into branched wormlike micelles (Figure 6c). This transition can be followed via a temperature sweep in a dynamic light scattering instrument (DLS, Figure 8d) after isolation of the population of the spherical micelles via filtration (pore size 220 nm). The isolated spherical micelles fuse into finite sized, larger aggregates upon reaching the cloud point during heating. When cooling down, the curve shows a strong hysteresis with larger, loosely bound aggregates being visible in the intermediate stage. After sufficient aging, the aggregate size is constant, sufficiently larger than before the heating cycle, and corresponds to a transition of the spherical micelles into branched wormlike micelles. Consequently, a clear and distinct change in the micelle architecture can be induced by the temperature cycle. The main transition happens during heating and is clearly assisted by the change (decrease) of the hydrophilic-to-hydrophobic ratio upon reaching the cloud point,

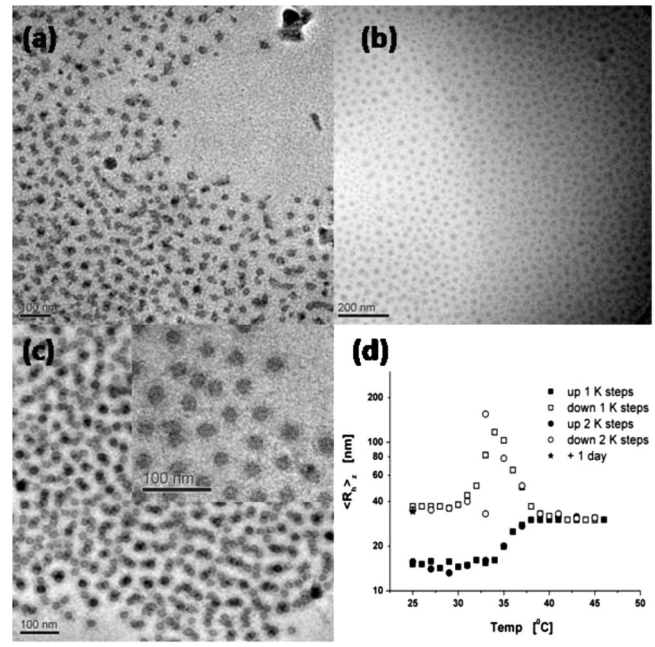

Figure 7. Cryo-TEM images of aggregates formed by PEO114-PnBuA105-PDEEAm181 after direct dissolution in water and stirring for 4 weeks (a), dialysis from dioxane into water (b), and a subsequent heating cycle of the aggregates (b) to 45 °C (c). Temperature-dependent DLS measurement for two different heating rates (squares = 1K steps, circles = 2K steps).

favoring formation of aggregates of lower curvature (i.e., wormlike micelles).[72−76] Utilization of the soft PnBuA provides the desired means for large-scale rearrangements in response to changes of the environmental conditions. Not only are the micelles able to change their corona structure (first level) due to the presence of thermo-responsive segments but also the overall structure of the micelles can be changed due to the low T_g of the hydrophobic block (second level). This represents a much

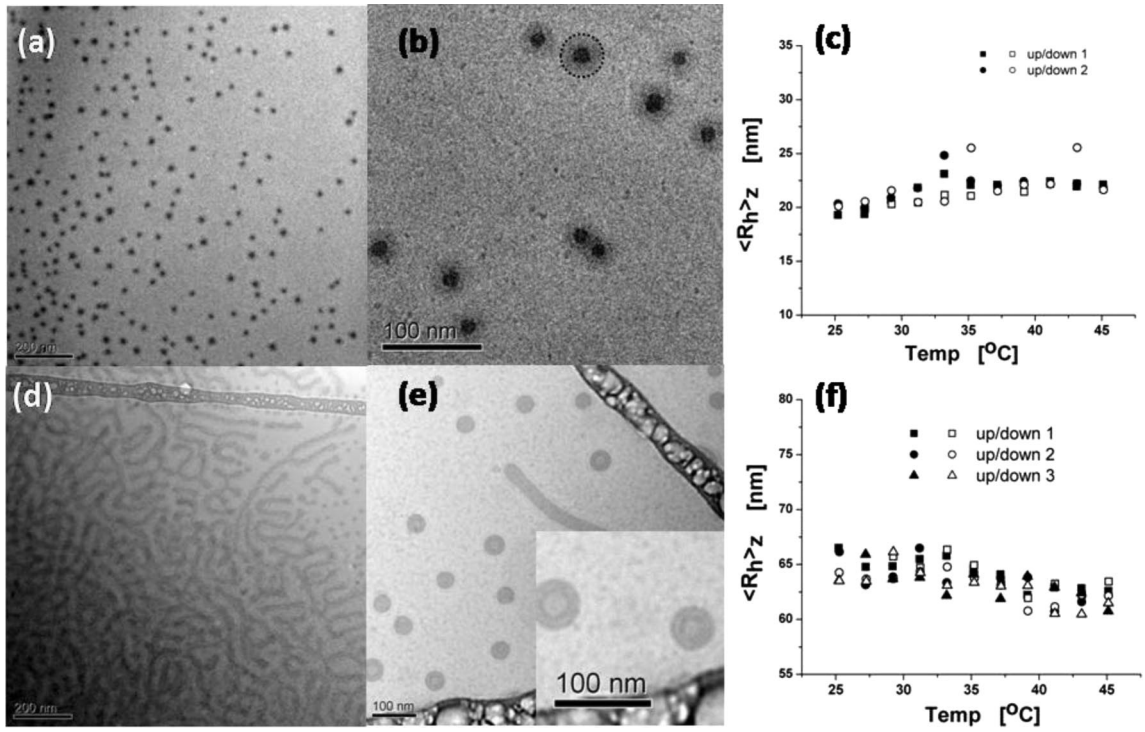

Figure 8. Cryo-TEM images of the major populations of aggregates found for PEO114-PnBuA105-PAAm103 (a, b), PEO114-PnBuA250-PAAm120 (d), and PEO114-PnBuA105-PHPMA101 (e). Repeated temperature sweep DLS measurements for PEO114-PnBuA105-PAAm103 (c) and PEO114-PnBuA105-PHPMA101 (f) after filtration with 220 nm filters.

higher degree of responsiveness that cannot be expected for high T_g polymers such as polystyrene or poly(2-vinylpyridine).The wormlike structure is stable upon further heating cycles in terms of the geometrical shape, indicating sufficient thermodynamic stability. Extension into longer cylindrical micelles can take place with further heating cycles. Hence, the spherical micelles are in a kinetically frustrated state, and the thermodynamically preferred architecture can be recovered via a heating cycle.

Similarly, cryo-TEM investigations of a block terpolymer with a significantly shorter hydrophobic block led to the images shown in Figure 7. The hydrophobic block length (PnBuA = 105 units) is decreased to a little less than one-half of the preceding polymer (PnBuA = 250 units). Direct dissolution into water yields small slightly ill-defined aggregates, meaning their cores are not entirely spherical, neither of a distinct other shape, e.g., disklike (Figure 7a). Dialysis leads to the observation of two distinct populations of spherical micelles (Figure 7b). The small spherical micelles fuse into larger spherical micelles after a heating cycle, representing the thermodynamically more stable structure (Figure 7c). The temperature ramp monitored by DLS (Figure 7d) shows first an increase of the hydrodynamic radius to a constant level and a further increase upon cooling. The first increase is presumably related to a fusion process of the small micelles and the second increase to an extension of the corona. The shape of the curve and extent of hysteresis is independent of the heating steps used, owing to a defined thermodynamic pathway of the transition. The transition from small micelles into larger ones again shows that aggregates of smaller curvature are more stable in water than what is obtained straight after dialysis.

Clearly, the shorter hydrophobic block of the latter polymer favors formation of spherical micelles, whereas the longer block leads to formation of aggregates of lower interfacial curvatures (rods and vesicles). This behavior can be understood in terms of adjusting the hydrophilic-to-hydrophobic balance.[72−76] Additionally, it can be concluded that the micelles obviously possess a dynamic character as they both undergo structural rearrangements and direct yet time-consuming dissolution in water. The occurrence of a certain aggregate shape depends on the preparation pathway and demonstrates the strong influence of kinetic effects in this system.

Due to the dynamic behavior in combination with incorporation of thermo-responsive segments, we expect an interesting behavior in terms of thermo-responsiveness of these structures. Indeed, the thermo-responsiveness and effect of repeated heating cycles on the aggregate structures and corona phase behavior will be addressed in a forthcoming publication.

In a last section we compare the influence of the last block on the morphology of the aggregates formed by PEO-*block*-PnBuA-*block*-PAAm and PEO-*block*-PnBuA-*block*-PHPMA (Figure 8). The upper two cryo-TEM micrographs (Figure 8a and 8b) show spherical micelles of PEO-*block*-PnBuA-*block*-PAAm with a short segment of the hydrophobic block (PnBuA = 105 units). The core−corona morphology is very visible in both micrographs and further highlighted by the circle in Figure 8b. Upon further increase of the hydrophobic block length (PnBuA = 250 units), while keeping the fraction of PAAm almost constant, a full transition to cylindrical micelles occurs (Figure 8d). This behavior is similar to the PNIPAAm and PDEAAm systems. However, extension using HPMA as the third block leads to the observation of very small vesicles and wormlike aggregates, even for very low fractions of PnBuA (PnBuA = 105 units, Figure 8e). This behavior is drastically different from the PNIPAAm and PDEAAm systems. Since the hydrophilic-to-hydrophobic balance is similar in all systems, the incompatibility of both end blocks starts playing a significant role. Aggregates of lower curvature are clearly preferred for rising incompatibility of the end blocks as the interface between the two end blocks can be minimized, i.e., by creating asymmetric vesicle walls. Although PEO and PAAm have shown to be incompatible in the case of the C3Ms,[53] the PHPMA/PEO system appears even more susceptible to formation of microphase segregation as concluded from the observation of the aggregates of lowest curvature. The colloidal

structures based on both PAAm and PHPMA block terpolymers are stable to several heating cycles, as shown by the temperature-dependent DLS measurements. Only slight expansions or contractions of the structures take place upon repeated heating. Consequently, the difference in aggregate structure does not originate from kinetic obstacles during the micelle preparation but from the chemically unlike end blocks and the different incompatibilities of them with PEO.

Conclusions

We present the synthesis of well-defined bis-hydrophilic block terpolymers possessing two hydrophilic end blocks via RAFT-mediated living/controlled radical polymerization. The strategy aims at a facile tunability of the corona structure and aggregate morphologies formed by these polymers.

Optimization of the synthesis of the PEO-based macro-CTAs allowed the easy and straightforward synthesis of amphiphilic PEO-*block*-PnBuA diblock copolymers of various compositions. The blocking efficiency is near quantitative, which makes complicated and time-consuming separation processes of homopolymer and diblock copolymer unnecessary. Similarly, extension with NIPAAm and DEAAm proceeds almost quantitatively as polymerizations of the diblock copolymers were stopped at moderate conversions in order to ensure a sufficient capping of the PEO-*block*-PnBuA with the CTA moiety. The block terpolymers with PDEAAm and PNIPAAm as well as the diblock copolymers were exhaustively characterized by SEC, MALDI-ToF, and NMR. They exhibit very low polydispersities, typically below 1.15. The reactions allow a full control of the hydrophilic and hydrophobic block length. For extension with AAm and HPMA, characterization remained challenging due to the strongly amphiphilic character of the polymers and the accompanying tendency to form aggregates in all kinds of solvents. Despite using several state-of-the-art SEC systems for amphiphilic block copolymers, a unimolecularly dissolved and well-separated species could not be characterized. The complete disappearance of the SEC peak related to the diblock copolymer precursor in conjunction with the controlled reaction kinetics and gradual change in the solution characteristics however strongly point toward a controlled chain extension.

Finally, the solution properties of the polymers in water are analyzed with respect to the corona block, hydrophilic-to-hydrophobic balance, and kinetics involved during dissolution and phase transitions. A direct dissolution of the polymers is possible due to the low glass-transition temperature of the hydrophobic block; however, the process requires weeks. The structures found for the polymers directly dissolved in water may be significantly different from the ones obtained by dialysis from a common solvent (dioxane, DMSO) into water, indicating a strong influence of the solvation pathway and kinetics. Direct dissolution in water leads to aggregates with lower curvature of the interface. Once dissolved in water, the aggregates can undergo structural transitions, i.e., from spherical into wormlike structures upon heating. The responsiveness to heat involves both the corona structure due to the presence of the LCST segments and the overall architecture of the micelle, which can rearrange because of the low T_g properties of the hydrophobic block, PnBuA. By tuning the hydrophilic-to-hydrophobic balance, a large variety of structures, i.e., spherical and wormlike micelles as well as vesicles, can be obtained. A strong effect of the chemistry of the third block and thus the interaction between the various blocks on the type of aggregates formed can be deduced. At similar composition the PAAm-based block terpolymers form spherical and wormlike micelles, whereas the PHPMA-based polymers form mainly vesicles. The terpolymers synthesized provide a novel platform for creation of multicompartment particles with tunable corona properties.

Acknowledgment. The authors are grateful for financial support from the Australian Research Council (ARC) and the Deutsche Forschungsgemeinschaft (DFG) for financial support in the form of a Linkage project. C.B.K. acknowledges receipt of an Australian Professorial Fellowship (ARC). We thank Mr. E. H. H. Wong, S. Edinger, D. Danz, and M. Schumacher for supporting mass spectrometry and size exclusion chromatography measurements. A.W. acknowledges support from the Bavarian Elite Support Program. Dr. L. Barner and Mr. I. Jacenyik are thanked for their excellent management of the CAMD facilities.

Supporting Information Available: ^{1}H NMR, ^{13}C NMR, 2D-HMBC NMR, SEC data, MALDI-ToF spectra of the block terpolymers, and discussion concerning the solubility behavior. This material is available free of charge via the Internet at http://pubs.acs.org.

References and Notes

(1) Rao, J.; Luo, Z.; Ge, Z.; Liu, H.; Liu, S. *Biomacromolecules* **2007**, *8*, 3871–3878.
(2) Wang, D.; Wu, T.; Wan, X.; Wang, X.; Liu, S. *Langmuir* **2007**, *23*, 11866–11874.
(3) Wang, D.; Yin, J.; Zhu, Z.; Ge, Z.; Liu, H.; Armes, S. P.; Liu, S. *Macromolecules* **2006**, *39*, 7378–7385.
(4) Cai, Y.; Armes, S. P. *Macromolecules* **2005**, *38*, 271–279.
(5) Liu, S.; Armes, S. P. *Langmuir* **2003**, *19*, 4432–4438.
(6) Weaver, J. V. M.; Armes, S. P.; Bütün, V. *Chem. Commun.* **2002**, 2122–2123.
(7) Liu, S.; Armes, S. P. *Angew. Chem., Int. Ed.* **2002**, *41*, 1413–1416.
(8) Zhang, L.; Bernard, J.; Davis, T. P.; Barner-Kowollik, C.; Stenzel, M. H. *Macromol. Rapid Commun.* **2008**, *29*, 123–129.
(9) Hsu, Y.-H.; Chiang, W.-H.; Chen, C.-H.; Chern, C.-S.; Chiu, H.-C. *Macromolecules* **2005**, *38*, 9757–9765.
(10) Topp, M. D. C.; Dijkstra, P. J.; Talsma, H.; Feijen, J. *Macromolecules* **1997**, *30*, 8518–8520.
(11) Gu, J.; Cheng, W.-P.; Liu, J.; Lo, S.-Y.; Smith, D.; Qu, X.; Yang, Z. *Biomacromolecules* **2008**, *9*, 255–262.
(12) Zhang, L.; Nguyen, T. L. U.; Bernard, J.; Davis, T. P.; Barner-Kowollik, C.; Stenzel, M. H. *Biomacromolecules* **2007**, *8*, 2890–2901.
(13) Sawant, R. M.; Hurley, J. P.; Salmaso, S.; Kale, A.; Tolcheva, E.; Levchenko, T. S.; Torchilin, V. P. *Bioconjugate Chem.* **2006**, *17*, 943–949.
(14) Giacomelli, C.; Le Men, L.; Borsali, R.; Lai-Kee-Him, J.; Brisson, A.; Armes, S. P.; Lewis, A. L. *Biomacromolecules* **2006**, *7*, 817–828.
(15) Zhang, W.; Shi, L.; Ma, R.; An, Y.; Xu, Y.; Wu, K. *Macromolecules* **2005**, *38*, 8850–8852.
(16) Rodriguez-Hernandez, J.; Lecommandoux, S. *J. Am. Chem. Soc.* **2005**, *127*, 2026–2027.
(17) Sfika, V.; Tsitsilianis, C.; Kiriy, A.; Gorodyska, G.; Stamm, M. *Macromolecules* **2004**, *37*, 9551–9560.
(18) Gil, E. S.; Hudson, S. M. *Prog. Polym. Sci.* **2004**, *29*, 1173–1222.
(19) Sumerlin, B. S.; Lowe, A. B.; Thomas, D. B.; McCormick, C. L. *Macromolecules* **2003**, *36*, 5982–5987.
(20) Yusa, S.; Shimada, Y.; Mitsukami, Y.; Yamamoto, T.; Morishima, Y. *Macromolecules* **2003**, *36*, 4208–4215.
(21) Liu, S.; Weaver, J. V. M.; Save, M.; Armes, S. P. *Langmuir* **2002**, *18*, 8350–8357.
(22) Roesler, A.; Vandermeulen, G. W. M.; Klok, H.-A. *Adv. Drug Delivery Rev.* **2001**, *53*, 95–108.
(23) Kataoka, K.; Harada, A.; Nagasaki, Y. *Adv. Drug Delivery Rev.* **2001**, *47*, 113–131.
(24) Hoffman, A. S.; Stayton, P. S. *Prog. Polym. Sci.* **2007**, *32*, 922–932.
(25) Bontempo, D.; Li, R. C.; Ly, T.; Brubaker, C. E.; Maynard, H. D. *Chem. Commun.* **2005**, 4702–4704.
(26) Rapoport, N. *Prog. Polym. Sci.* **2007**, *32*, 962–990.
(27) Walther, A.; André, X.; Drechsler, M.; Abetz, V.; Müller, A. H. E. *J. Am. Chem. Soc.* **2007**, *129*, 6187–6198.
(28) Walther, A.; Müller, A. H. E. *Soft Matter* **2008**, *4*, 663–668.
(29) Li, Z.; Kesselman, E.; Talmon, Y.; Hillmyer, M A.; Lodge, T. P. *Science* **2004**, *306*, 98–101.
(30) Li, Z.; Hillmyer, M. A.; Lodge, T. P. *Langmuir* **2006**, *22*, 9409–9417.
(31) Cui, H.; Chen, Z.; Zhong, S.; Wooley, K. L.; Pochan, D. J. *Science* **2007**, *317*, 647–650.
(32) Cui, H.; Chen, Z.; Wooley, K. L.; Pochan, D. J. *Macromolecules* **2006**, *39*, 6599–6607.
(33) Li, Z.; Chen, Z.; Cui, H.; Hales, K.; Qi, K.; Wooley, K. L.; Pochan, D. J. *Langmuir* **2005**, *21*, 7533–7539.
(34) Wang, X.; Guerin, G.; Wang, H.; Wang, Y.; Manners, I.; Winnik, M. A. *Science* **2007**, *317*, 644–647.

(35) Li, Z.; Hillmyer, M. A.; Lodge, T. P. *Macromolecules* **2006**, *39*, 765–771.
(36) Lodge, T. P.; Rasdal, A.; Li, Z.; Hillmyer, M. A. *J. Am. Chem. Soc.* **2005**, *127*, 17608–17609.
(37) Kubowicz, S.; Baussard, J.-F.; Lutz, J.-F.; Thuenemann, A. F.; von Berlepsch, H.; Laschewsky, A. *Angew. Chem., Int. Ed.* **2005**, *44*, 5262–5265.
(38) Lutz, J.-F.; Laschewsky, A. *Macromol. Chem. Phys.* **2005**, *206*, 813–817.
(39) Willet, N.; Gohy, J.-F.; Auvray, L.; Varshney, S.; Jerome, R.; Leyh, B. *Langmuir* **2008**, *24*, 3009–3015.
(40) Willet, N.; Gohy, J.-F.; Lei, L.; Heinrich, M.; Auvray, L.; Varshney, S.; Jerome, R.; Leyh, B. *Angew. Chem., Int. Ed.* **2007**, *46*, 7988–7992.
(41) Khanal, A.; Inoue, Y.; Yada, M.; Nakashima, K. *J. Am. Chem. Soc.* **2007**, *129*, 1534–1535.
(42) Zhang, W.; Jiang, X.; He, Z.; Xiong, D.; Zheng, P.; An, Y.; Shi, L. *Polymer* **2006**, *47*, 8203–8209.
(43) Li, G.; Shi, L.; An, Y.; Zhang, W.; Ma, R. *Polymer* **2006**, *47*, 4581–4587.
(44) Lei, L.; Gohy, J.-F.; Willet, N.; Zhang, J.-X.; Varshney, S.; Jerome, R. *Polymer* **2004**, *45*, 4375–4381.
(45) Lei, L.; Gohy, J.-F.; Willet, N.; Zhang, J.-X.; Varshney, S.; Jerome, R. *Macromolecules* **2004**, *37*, 1089–1094.
(46) Gohy, J.-F.; Willet, N.; Varshney, S.; Zhang, J.-X.; Jerome, R. *Angew. Chem., Int. Ed.* **2001**, *40*, 3214–3216.
(47) Liu, F.; Eisenberg, A. *J. Am. Chem. Soc.* **2003**, *125*, 15059–15064.
(48) Stoenescu, R.; Graff, A.; Meier, W. *Macromol. Biosci.* **2004**, *4*, 930–935.
(49) Stoenescu, R.; Meier, W. *Chem. Commun.* **2002**, 3016–3017.
(50) Charlaganov, M.; Borisov, O. V.; Leermakers, F. A. M. *Macromolecules* **2008**, *41*, 3668–3677.
(51) Li, G.; Shi, L.; Ma, R.; An, Y.; Huang, N. *Angew. Chem., Int. Ed.* **2006**, *45*, 4959–4962.
(52) Ma, R.; Wang, B.; Xu, Y.; An, Y.; Zhang, W.; Li, G.; Shi, L. *Macromol. Rapid Commun.* **2007**, *28*, 1062–1069.
(53) Voets, I. K.; de Keizer, A.; De Waard, P.; Frederik, P. M.; Bomans, P. H. H.; Schmalz, H.; Walther, A.; King, S. M.; Leermakers, F. A. M.; Cohen Stuart, M. A. *Angew. Chem., Int. Ed.* **2006**, *45*, 6673–6676.
(54) Halperin, A. *J. Phys. (Paris)* **1988**, *49*, 131.
(55) Chiefari, J.; Chong, Y. K.; Ercole, F.; Krstina, J.; Jeffery, J.; Le, T. P. T.; Mayadunne, R. T. A.; Meijs, G. F.; Moad, C. L.; Moad, G.; Rizzardo, E.; Thang, S. H. *Macromolecules* **1998**, *31*, 5559–5562.
(56) Barner, L.; Davis, T. P.; Stenzel, M. H.; Barner-Kowollik, C. *Macromol. Rapid Commun.* **2007**, *28*, 539–559.
(57) Perrier, S.; Takolpuckdee, P. *J. Polym. Sci., Part A: Polym. Chem.* **2005**, *43*, 5347–5393.
(58) Hong, C.-Y.; Pan, C.-Y. *Macromolecules* **2006**, *39*, 3517–3524.
(59) Scales, C. W.; Vasilieva, Y. A.; Convertine, A. J.; Lowe, A. B.; McCormick, C. L. *Biomacromolecules* **2005**, *6*, 1846–1850.
(60) Rihova, B.; Kubackova, K. *Curr. Pharm. Biotechnol.* **2003**, *4*, 311–322.
(61) Konak, C.; Oupicky, D.; Chytry, V.; Ulbrich, K.; Helmstedt, M. *Macromolecules* **2000**, *33*, 5318–5320.
(62) Bang, J.; Kim, S. H.; Drockenmuller, E.; Misner, M. J.; Russell, T. P.; Hawker, C. J. *J. Am. Chem. Soc.* **2006**, *128*, 7622–7629.
(63) Stenzel, M. H. *Complex Architecture Design via the RAFT Process: Scope, Strengths and Limitations in Handbook of RAFT Polymerization*; Barner-Kowollik, C., Ed.; Wiley-VCH: Weinheim, Germany, 2008, pp 315−367.
(64) Li, Y.; Lokitz, B. S.; McCormick, C. L. *Macromolecules* **2006**, *39*, 81–89.
(65) Barner-Kowollik, C.; Davis, T. P.; Stenzel, M. H. *Polymer* **2004**, *45*, 7791–7805.
(66) Vana, P.; Albertin, L.; Barner, L.; Davis, T. P.; Barner-Kowollik, C. *J. Polym. Sci., Part A: Polym. Chem.* **2002**, *40*, 4032–4037.
(67) Barner-Kowollik, C.; Quinn, J. F.; Morsley, D. R.; Davis, T. P. *J. Polym. Sci., Part A: Polym. Chem.* **2001**, *39*, 1353–1365.
(68) Barner-Kowollik, C.; Buback, M.; Charleux, B.; Coote, M. L.; Drache, M.; Fukuda, T.; Goto, A.; Klumperman, B.; Lowe, A. B.; McLeary, J. B.; Moad, G.; Monteiro, M. J.; Sanderson, R. D.; Tonge, M. P.; Vana, P. *J. Polym. Sci., Part A: Polym. Chem.* **2006**, *44*, 5809–5831.
(69) Yu, K.; Zhang, L.; Eisenberg, A. *Langmuir* **1996**, *12*, 5980–5984.
(70) Zhang, L.; Eisenberg, A. *Polym. Adv. Technol.* **1998**, *9*, 677–699.
(71) Zhang, L.; Eisenberg, A. *Macromolecules* **1999**, *32*, 2239–2249.
(72) Zhang, L.; Eisenberg, A. *J. Am. Chem. Soc.* **1996**, *118*, 3168–81.
(73) Jain, S.; Bates, F. S. *Science* **2003**, *300*, 460–464.
(74) Zhang, L.; Eisenberg, A. *Science* **1995**, *268*, 1728–1731.
(75) Walther, A.; Goldmann, A. S.; Yelamanchili, R. S.; Drechsler, M.; Schmalz, H.; Eisenberg, A.; Müller, A. H. E. *Macromolecules* **2008**, *41*, 3254–3260.
(76) Rodriguez-Hernandez, J.; Checot, F.; Gnanou, Y.; Lecommandoux, S. *Prog. Polym. Sci.* **2005**, *30*, 691–724.

MA801215Q